بسم الله الرحمن الرحيم

Sudan University of Science and Technology

College of Graduate Studies

كلية الدراسات العليا

Estimation of Effective Radiation Dose During Brain Computed Tomography

تقويم الجرعة الإشعاعية الفعالة أثناء إختبارات الأشعة المقطعية المحوسبة للدماغ

A Thesis Submitted in Partial Fulfillment of the Requirements for the M.Sc. Degree in Medical Physics

By:

Abubaker Alsaid Ahmed Alhaj

Supervisor:

Dr. Suhaib Mohamedsalih Ahamed Alameen

October – 2018

الآيـــــــة

قَالَ تَعَالَىٰ: ﴿هُوَ ٱلَّذِى جَعَلَ ٱلشَّمۡسَ ضِيَآءً وَٱلۡقَمَرَ نُورًا وَقَدَّرَهُۥ مَنَازِلَ لِتَعۡلَمُواْ عَدَدَ ٱلسِّنِينَ وَٱلۡحِسَابَۚ مَا خَلَقَ ٱللَّهُ ذَٰلِكَ إِلَّا بِٱلۡحَقِّۚ يُفَصِّلُ ٱلۡأٓيَٰتِ لِقَوۡمٍ يَعۡلَمُونَ ۝٥﴾

سورة يونس الآية (5)

Dedication

I dedicate this work To My Parents for Their Patience

and Encouragement.

To My Brothers and Sister for Their Support.

To My Friends and teachers

Acknowledgements

First, my acknowledgement and gratefulness to the God to give as this mind.

I would like to express my deepest gratitude to my supervisor Dr. Suhaib Mohamedsalih Ahamed for his guidance, without his help this work could not have accomplished in this way. Also, my deep thanks to my friend Ms. Mustafa Awad who was support and help me when I was need to him. Also, my thanks extended to my classmate Mohamed H. Elamir for help me when I was need to him. Also, my thanks the families of the four hospitals in Khartoum state from which the data of this study was collected. Finally, I would like to sincerely thank my family for their consistent mental support.

Abstract

CT is an important diagnostic tool in modern healthcare; however, CT is a high radiation exposure modality compared to conventional X-ray devices. This study was carried out to estimate radiation dose received by the patients during brain CT scan.

The total data in this study was 117 adult patients undergoing brain CT scan by two different CT scanners (Toshiba 64 & 16 slice) in four hospitals in Khartoum state during April to August 2018, were collect scan parameters, CTDI and DLP and evaluate effective dose by using CT expo version 2.5 software.

The results of this study revealed that the mean of effective dose in CT Toshiba 64 slice and CT Toshiba 16 slice was (4.6 ± 0.9) mSv, (2.8 ± 0.5) mSv respectively, and the mean of sensitive organ dose (i.e., eye lens) for Toshiba 64 & 16 slice was (82.8 ± 0.6) mSv, (53.2 ± 0.4) mSv respectively.

This study concluded that the mean of radiation dose received by CT scanner 64 slice is higher than CT scanner 16 slice, this difference refers to the difference in protocols.

المستخلص

جهاز الأشعة المقطعية (CT) هو أداة تشخيصية مهمة في مجال الرعاية الصحية الحديثة. ومع ذلك ، إن استخدام جهاز الاشعة المقطعية يعطى المرضى جرعة اشعاعية عاليه مقارنة مع مختلف انواع اجهزه الاشعة السينية التقليدية.

وقد أجريت هذه الدراسة لتقدير الجرعة الإشعاعية للمرضى الذين خضعوا لفحص الدماغ عن طريق الأشعة المقطعية. مجموع المرضى في هذه الدراسة كان 117 مريض من البالغين الذين خضعوا لفحص الدماغ عن طريق الأشعة المقطعية بواسطة نوعين مختلفين من أجهزة الأشعة المقطعية هما (توشيبا 64 شريحة) و (توشيبا 16 شريحة) ، تم جمع معاملات الفحص ومعاملات لها علاقة بالجرعة الإشعاعية (CTDI, DLP) ، ومن ثم تم تقييم الجرعة الإشعاعية الفعالة عن طريق برنامج معالج البيانات CT Expo.

نتائج هذه الدراسة أظهرت أن متوسط الجرعة الإشعاعية الفعالة في الجهاز (توشيبا 64 شريحة) و (توشيبا 16 شريحة) هي (0.9 ± 4.6) ، (0.5 ± 2.8) mSv علي التوالي.

وأن متوسط الجرعة الإشعاعية الواصلة للأعضاء الأكثر حساسية للإشعاع مثل: عدسة العين في الجهازين توشيبا 64 و توشيبا 16 شريحة (0.6 ± 82.8) mSv ، (0.4 ± 53.2) mSv على التوالي.

وجد في هذه الدراسة أن متوسط الجرعة الإشعاعية الفعالة الواصلة للمرضى بواسطة جهاز الأشعة المقطعية توشيبا 64 شريحة هي أعلى من الواصلة بواسطة الجهاز توشيبا 16 شريحة.

Table of contents

الآية	I
Dedication	II
Acknowledgements	III
Abstract	IV
المستخلص	V
Table of contents	VI
List of Tables	IX
List of Figures	XI
List of Abbreviations	XII
Chapter One – Introduction	
1.1. Introduction	1
1.2. Problem of the study	4
1.3. Objectives of the study	4
1.3.1. General objectives	4
1.3.2. Specific objectives	4
1.4. Outline of the study	4
Chapter Two - Theoretical Background	
2.1. Computed Tomography Imaging	9
2.2. CT generations	10
2.2.1. First Generation: Rotate/translate, Pencil beam	10
2.2.2. Second Generation: Rotate/translate, Narrow Fan Beam	11
2.2.3. Third Generation: Rotate/Rotate, Wide Fan Beam	12
2.2.4. Fourth Generation (Rotate/Stationary)	12
2.2.5. Fifth Generation (Stationary/Stationary)	12
2.2.6. Sixth Generation: Helical	13
2.2.7. Seven Generation: Multiple Detector Array	13
2.3. Components of the CT scan	14
2.3.1. Gantry and table	14
2.3.2 The X ray tube and generator	15

2.3.3. Collimation and filtration	15
2.3.4. Detectors	15
2.4. Detector pitch and collimation pitch	16
2.5. Data Acquisition System (DAS)	18
2.6. Dosimetric quantities and units	19
2.6.1. particle fluence	19
2.6.2. Energy Fluence (ψ)	20
2.6.3. Kerma(K)	20
2.6.4. Absorbed Dose	21
2.7. Quantities for CT Dosimetry	22
2.7.1. Computed Tomography Dose Index (CTDI)	22
2.7.2. $CTDI_{FAD}$	23
2.7.3. $CTDI_{100}$	23
2.7.4. Weighted $CTDL_W$	24
2.7.5. Volume $CTDI_{VOL}$	24
2.7.6. Dose Length Product (DLP)	26
2.8. System of Radiological Protection	27
2.8.1. Justification	27
2.8.2. Optimization	27
2.8.3. Dose limitation	27
2.9. Radiation quantities	28
2.9.1. Organ dose	28
2.9.2. Equivalent Dose	29
2.9.3. Effective dose	30
2.9.3.1 Effective Dose (E) in CT	30
2.10. Literature review	33
Chapter Three - Materials & Method	
3.1. Materials	38
3.1.1 Machines	38
3.1.2 Population	38
3.2. Method	38

3.2.1 Data collection	38
3.2.2. Dosimetric calculations	38
3.2.2.1 CT-Expo V 2.5 software	39
3.2.3 Data Analysis	39
Chapter Four – Results	
4.1. Results	40
Chapter five - Discussion, Conclusion and Recommendations	
5.1. Discussion	51
5.2. Conclusion	54
5.3. Recommendations	55
5.4 Appendix	56
References	55

List of Tables

Table NO	Item	Page NO
2.1	Radiation weighting factors in publication ICRP 60 and Q in publication ICRP	30
2.2	Tissue weighting factors for different organs	30
4.1	summaries the characteristic statistics parameters for the hospital (A) from The CT scanner Toshiba model Acquilion (64-slice)	40
4.2	summaries the characteristic statistics parameters for the hospital (A) from The CT scanner Toshiba model Acquilion (64-slice), for male	40
4.3	summaries the characteristic statistics parameters for the hospital (A) from The CT scanner Toshiba model Acquilion (64-slice), for female	41
4.4	comparison of (E) between male and female from Toshiba CT scanner model Acquilion (64-slice) for the hospital (A)	41
4.5	summaries the characteristic statistics parameters for the hospital (B) from The CT scanner Toshiba model Acquilion (64-slice)	42
4.6	summaries the characteristic statistics parameters for the hospital (B) from The CT scanner Toshiba model Acquilion (64-slice) for male	42
4.7	summaries the characteristic statistics parameters for the hospital (B) from The CT scanner Toshiba model Acquilion (64-slice) for female	43
4.8	comparison of (E) between male and female from Toshiba CT scanner model Acquilion (64-slice) for the hospital (B)	43
4.9	summaries the characteristic statistics parameters for the hospital (C) from The CT scanner Toshiba model Acquilion (16-slice)	44
4.10	summaries the characteristic statistics parameters for the hospital (C) from The CT scanner Toshiba model Acquilion (16-slice) for male	44

4.11	summaries the characteristic statistics parameters for the hospital (C) from The CT scanner Toshiba model Acquilion (16-slice) for female	45
4.12	comparison of (E) between male and female from Toshiba CT scanner model Acquilion (16-slice) for the hospital (C)	45
4.13	summaries the characteristic statistics parameters for the hospital (D) from The CT scanner Toshiba model Acquilion (16-slice)	46
4.14	summaries the characteristic statistics parameters for the hospital (D) from The CT scanner Toshiba model Acquilion (16-slice) for male	46
4.15	summaries the characteristic statistics parameters for the hospital (D) from The CT scanner Toshiba model Acquilion (16-slice) for female	47
4.16	comparison of (E) between male and female from Toshiba CT scanner model Acquilion (16-slice) for the hospital (D)	47
4.17	The mean of CTDI, DLP and E in this study and compare with other country and EC reference dose	48
4.18	organ dose estimated from The CT scanner Toshiba model Acquilion (64-slice)	49
4.19	organ dose estimated from The CT scanner Toshiba model Acquilion (16-slice)	50

List of figures

Figures No	Item	Page NO
2.1	First – Generation (rotate/translate) Computed tomography	10
2.2	The difference between pencil beam, fan beam, and open beam geometry	11
2.3	Helical Computed Tomography Scanners	13
2.4	Detector pitch and Collimation Pitch	17
4.1	Compare the effective dose between the four centers	48

List of Abbreviations

CT	Computed Tomography
ALARA	As Low As Reasonably Achievable
ICRP	International Commission on Radiological Protection
DAS	Data Acquisition System
MSAD	Multiple Scan Average Dose
MDCT	Multi Detector Computed Tomography
CTDI	Computed Tomography dose index
CTDI100	Computed Tomography dose index, for a100 mm length pencil ion chamber
CTDIvol	Volumetric Computed Tomography dose index
CTDIw	Weighted Computed Tomography dose index
DLP	Dose Length Product
E	Effective Dose
D	Absorbed Dose
FDA	Food and Drug Administration
W_R	Radiation Weighting Factor
W_T	Tissue Weighting Factor
KERMA	Kinetic Energy Released per unit Mass
Kvp	Kilo Voltage Peak
mAs	Mile Ampere Second
NRPB	National Radiological Protection Board
FOV	Feld of View
ROI	Region of Interest
ESD	Entrance Surface Dose
D_T	Organ Dose
H_T	Equivalent Dose
MeV	Mega electron Volt
mSv	Mile Sievert
EC	European Commission
AEC	Automatic Exposure Control

CHAPTER ONE

INTRODUCTION

Chapter One

Introduction

1.1. Introduction

Computed tomography (CT) is in its fourth decade of clinical use and has proved in valuable as a diagnostic tool for many clinical applications, from cancer diagnosis to trauma to osteoporosis screening. CT was the first imaging modality that made it possible to probe the inner depths of the body, slice by slice. Since 1972, when the first head CT scanner was introduced, CT has matured greatly and gained technological sophistication. Concomitant changes have occurred in the quality of CT images. The first CT scanner, an EMI Mark 1, produced images with 80 X 80-pixelresolution (3-mm pixels), and each pair of slices required approximately 4.5 minutes of scan time and 1.5 minutes of reconstruction time. Because of the long acquisition times required for the early scanners and the constraints of cardiac and respiratory motion, it was originally thought that CT would be practical only for head scans. CT is one of the many technologies that was made possible by the invention of the computer.(Bushberg et al., 2003)

The clinical potential of CT became obvious during its early clinical use, and the excitement forever solidified the role of computers in medical imaging. Recent advances in acquisition geometry, detector technology, multiple detector arrays, and x-ray tube design have led to scan times now measured in fractions of second. Modern computers deliver computational power that allows reconstruction of the image data essentially in real time. The invention of the CT scanner earned God Frey Hounsfield of Britain and Allan Cormack of the United States the Nobel Prize for Medicine in 1979.(Bushberg et al., 2003)

CT scanner technology today is used not only in medicine but in many other industrial applications, such as nondestructive testing and soil core analysis. (Bushberg et al., 2003)

Computed tomography (CT) is an influential diagnostic instrument in new-fashioned healthcare. However, CT is a high radiation exposure formalism in compare to imitative X-ray devices. The number of examinations has been continuously increased and, now, CT is a major source of exposure in diagnostic X-rays for populations. In 1989, CT accounted for about 4% of diagnostic radiology examinations performed in the UK, contributing 40% of the collective population dose from medical radiation. (Sadri et al., 2013)

An importance of the profit of CT examinations, it has become the gold standard for assortment of clinical indications, such as diagnosing certain cancers, surgical striping, and detecting internal injuries and bleeding in trauma cases. (Association, 2006) Diagnostic significance of CT examinations is noticeable, so the increase of examination frequency is justified. According to the International Commission on Radiological Protection (ICRP) dose limits should not be applied for medical exposures either diagnostic or therapy, because patients have direct benefit from the exposure. However according to the basic principles of radiation protection the medical diagnostic procedures should be optimized and unjustified exposures should be minimized. (Ali, 2005) The use of computed tomography vouchsafes patients more radiation dose than imitative x-ray imaging modalities. Patients are exposed to more dose which may result in unwilled health effects. health care providers require to be able to evaluate and track the dose these patients obtain from their CT scan. (Prins et al., 2011)

CT examination is a high-radiation-dose imaging technique using x-rays. Radiation has well-known stochastic and deterministic effects on body organs. Many different types of multi detector CT (MDCT) can be found in the market and even within the same imaging center today.(Tan et al., 2009)

Ideally, all scanning should be performed on the most efficient scanner that offers the best image quality at the lowest radiation dose. However, logistic and workflow segregation problems related to infection control may not allow this. To our knowledge, there has been no study to date that compares the radiation dose delivered to the eye lens by 16- and 64-section (MDCT). (Tan et al., 2009)

The eye lens is one of the most radiosensitive tissues. According to 1990 recommendations of the ICRP, the thresholds in a single brief exposure for detectable opacities and visual impairment (cataract) are 0.5–2.0 and 5.0 Sv, respectively. In highly fractionated or protracted exposures, the threshold is 5 Sv for detectable opacities and 8 Sv for cataracts. However, a number of recent studies have supported lower thresholds for radiation-induced lens injuries. Some authors have suggested that the risk of cataract increases with increased radiation dose without a threshold. Given these data, the ICRP referred to the need for a detailed revaluation of the radio sensitivity of the lens. (Suzuki et al., 2010)

1.2. Problem of the study

Due to use CT scanning patients are exposed to more doses which may result in unintended health effects, to avoid unnecessary of high dose to the patients need to estimate the patient dose to control the dose and achieve the minimize the patient dose without reduce image quality and compare this dose between different MDCT, and establish their protocol without following and activate the AEC choice, and without following the international recommendations and IAEA, ICRP guidelines of dose optimizations.

1.3. Objectives of the study

1.3.1. General objective:

Estimation of patient effective dose and organ dose during brain compute tomography examinations.

1.3.2. Specific objectives:

- To calculate of effective dose for patients during CT brain examinations.
- To evaluation of patient dose from CT 64 & 16 slice.
- To evaluation of dose for sensitive organs from both modalities (64 & 16 slice).
- To compare of Effective and organ doses from 16 and 64 CT machines.
- To compare our results with national and international studies.

1.4. Outline of the study

This chapter is comprise general introduction to the computed tomography, System of Radiological Protection and the objectives of this study. Chapter tow is comprise theoretical background about

computed tomography, CT components, CT generations, dosimetric quantities and units, and radiation protection quantities. The published literature and studies done on the research subject were reviewed in this chapter.

Chapter Three describes the materials and methods used in this study to assess the eye lens radiation dose. Chapter four consists of presentation of the results. Chapter five consists of discussion of the results, conclusion and recommendations that had been derived out from the research.

CHAPTER TWO

THEORETICAL BACKGROUND

Chapter Two

Theoretical Background

2.1. Computed Tomography Imaging:

Tomography literally means a slice view of the patient although the term sections imaging is now preferred. Tomography is an x-ray imaging technique that produces sectional views of the patient in plane parallel to the table top on which the patient is lying. The contrast demonstrated by this technique is poor because of the influence of overlying tissues. Computed tomography (CT) generates images in trans axial sections. Unlike linear tomography CT images are not influenced by the properties of neighboring regions of the body. They are therefore able to display levels of contrast that truly represent the subject contrast within the imaging section with only limitations being imposed by the width. (Allisy-Roberts and Williams, 2007)

Computed tomography (CT)developed from an X ray modality that was limited to axial imaging of the brain in neuroradiology into a versatile 3-D whole body imaging modality for a wide range of applications, including oncology, vascular radiology, cardiology, traumatology and interventional radiology. CT is applied for diagnosis and follow-up studies of patients, for planning of radiotherapy, and even for screening of healthy subpopulations with specific risk factors. Computed Tomography (CT) is a radiologic modality that supplies clinical information in the detection, differentiation, and demarcation of disease. It is the primary diagnostic modality for a variety of presenting problems and is widely accepted as a supplement to other imaging techniques. CT is a form of medical imaging that requires the exposure of patients to ionizing radiation. (Dance et al., 2014)

During a CT scan a rotating source passes x-rays through a patient's body to produce several cross-sectional images of a particular area. These two-dimensional images can also be digitally combined to produce a single three-dimensional. (Ali, 2005)

2.2. CT generations

2.2.1. First Generation: Rotate/translate, Pencil beam

CT scanners represent a marriage of diverse technologies, including computer hardware, motor control systems, x-ray detectors, sophisticated reconstruction algorithms, and x-ray tube/generator systems. The first generation of CT scanners employed a rotate/translate, pencil beam system. Only two x-ray detectors were used, and they measured the transmission of x-rays through the patient for two different slices. The acquisition of the numerous projections and the multiple rays per projection required that the single detector for each CT slice be physically moved throughout all the necessary positions. (Bushberg et al., 2003)

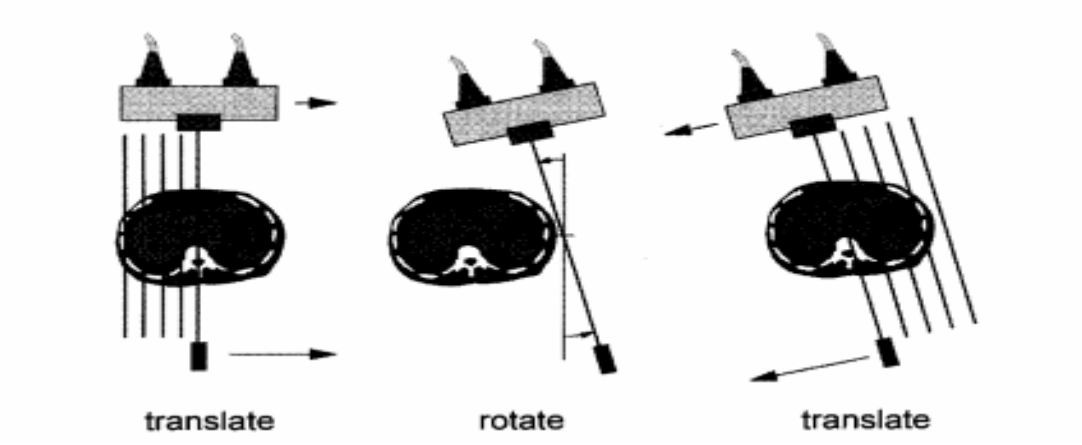

Fig (2.1) *First-generation (rotate/translate) computed tomography CT.*

The x-ray tube and a single detector translate across the field of view, producing a series of parallel rays.

The system then rotates slightly and translates back across the field of view, producing ray measurements at a different angle. This process is repeated at 1-degree intervals over 180 degrees, resulting in the complete CT data set**.**(Bushberg et al., 2003)

2.2.2. Second Generation: Rotate/translate, Narrow Fan Beam

The next incremental improvement to the CT scanner was the incorporation of a linear array of 30 detectors. This increased the utilization of the x-ray beam by 30times, compared with the single detector used per slice in first-generation systems. A relatively narrow fan angle of 10 degrees was used. In principle, a reduction in scan time of about 30-fold could be expected. However, this reduction time was not realized, because more data were acquired to improve image quality.

The shortest scan time with a second-generation scanner was 18 seconds per slice, 15 times faster than with the first-generation system. Incorporating an array of detectors, instead of just two, required the use of an arrow fan beam of radiation. Although a narrow fan beam provides excellent scatter rejection compared with plain film imaging, it does allow more scattered radiation to be detected than was the case with the pencil beam used in first-generation CT.(Bushberg et al., 2003)

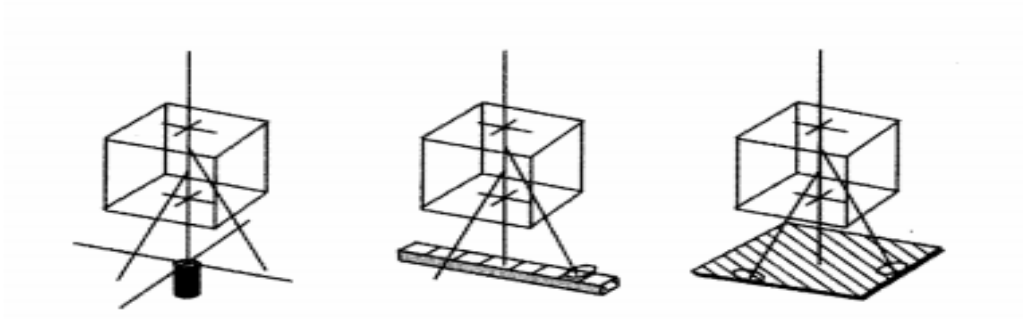

Pencil beam Fan beam Open beam

Fig (2.2) *The difference between pencil beam, fan beam, and open beam geometry in terms of scatter detection.(Bushberg et al., 2003)*

2.2.3. Third Generation: Rotate/Rotate, Wide Fan Beam

The translational motion of first- and second-generation CT scanners was a principal obstacle to fast scanning. At the end of each translation, the movement of the x-ray tube system had to be hinder, the whole system rotated, and the translational movement restarted. The attaining prosperity of CT as a clinical modality in its infancy gave craftsman reason to explore more capable, but more costly approaches to the scanning geometry the motion of third-generation CT is "Rotate/Rotate" referring to the motion of the x-ray tube and the movement of the detector array. By elimination of the translational motion the scan time is decreased virtually. The early third-generation scanners could deliver scan times shorter than 5 seconds. Newer systems have scan times of one half second. The development from first- to second- and second- to third-generation scanners included radical enhancement with each step. Developments of the fourth- and fifth-generation scanners led not only to some improvement's compromises in clinical CT images, compared third-generation scanners but also to some indeed, rotate/rotate scanners are still as viable today as they were when they were introduced in 1975. The

features of third- and fourth-generation CT should be compared by the reader, because each offers some benefits but also some tradeoffs.(Bushberg et al., 2003)

2.2.4. Fourth Generation (Rotate/Stationary)

Third-generation scanners suffered from the significant problem of ring artifacts, and in the late 1970s fourth-generation scanners were designed specifically to address these artifacts.

It is never possible to have a large number of detectors in perfect balance with each other, and this was especially true 25 years ago. Each detector and its associated electronics has a certain amount of drift, causing the signal levels from each detector to shift over time.

The rotate/rotate geometry of third-generation scanners leads to a situation in which each detector is responsible for the data corresponding to a ring in the image. Detectors toward the center of the detector array provide data in the reconstructed image in a ring that is small in diameter, and more peripheral detectors contribute to larger diameter rings. Fourth-generation CT scanners were designed to overcome the problem of ring artifacts. With fourth-generation scanners, the detectors are removed from the rotating gantry and are placed in a stationary 360-degree ring around the patient requiring many more detectors. Modern fourth-generation CT systems use about 4,800 individual detectors. Because the x-ray tube rotates and the detectors are stationary, fourth-generation CT is said to use a rotate/stationary geometry.(Bushberg et al., 2003)

2.2.5. Fifth Generation (Stationary/Stationary)

A new CT scanner has been promoted specifically for cardiac tomographic imaging. This "cine-CT" scanner does not use a imitative x-ray tube; instead, a large arc of tungsten encircles the patient and He's directly positioned in the other side to the detector ring.(Bushberg et al., 2003)

2.2.6. Sixth Generation: Helical

Third-generation and fourth-generation CT geometries solved the mechanical inertia limitations involved in acquisition of the individual projection data by eliminating the translation motion used in first- and second-generation scanners.

However, the gantry had be stopped after each slice was acquired, because the detectors (in third-generation scanners) and the x-ray tube (in third- and fourth-generation machines) had to be connected by wires to the stationary scanner electronics. Helical CT acquire data while the table is moving; as a result, the x-ray source moves in a helical pattern around the patient being scanned.(Bushberg et al., 2003)

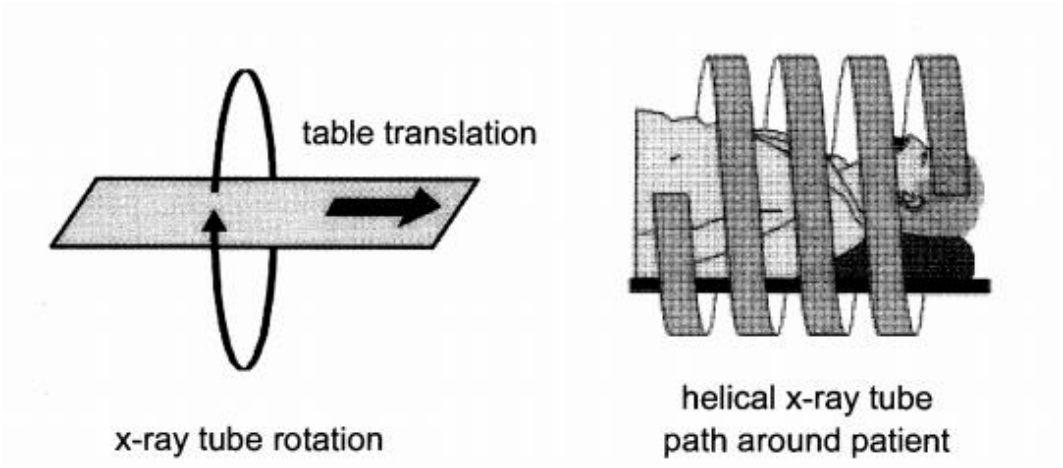

Fig (2.3) *helical computed tomographic scanners*.

The x-ray tube rotates around the patient while the patient and the table are translated through the gantry.(Bushberg et al., 2003)

2.2.7. Seven Generation: Multiple Detector Array

X-ray tubes designed for CT have effective heat storage and cooling capacity although the immediate production of x-rays is limited by the physics governing x-ray production. An approach to overcoming x-ray tube output limitations is to make better use of the x-rays that are produced by the x-ray tube. The collimator spacing is wider when multiple detector arrays are utilized and therefore more of the x-rays that are produced by the x-ray tube are used in producing image data. With conventional, single detector array scanners, opening up the collimator increases the slice thickness which is good for improving the utilization of the x-ray beam but decreases spatial resolution in the slice thickness dimension. The slice thickness is not determined by the collimator but by the detector size. This represents a significant shift in CT technology.

The elasticity of CT acquirement protocols and the more efficiency ensuing from multiple detector array CT scanners provides for better patient imaging, however, the number of parameters involved in the CT acquisition protocol is increased as well.(Bushberg et al., 2003)

2.3. Components of the CT scan

2.3.1. Gantry and table

The gantry contains all the system components that are required to record transmission profiles of the patient. since transmission profiles have to be recorded at different angles, these components are mounted on a support within the gantry that can be rotated. the X ray tube with

high voltage generator and tube cooling system, the collimator, the beam shaping filters, the detector arc and the data acquisition system are all mounted on this support. the engineering of these components is complex, since they need to be able to withstand the strong centrifugal force that occurs during the fast rotation of the gantry. forces of several tens of g arise for rotation times of the order of 0.25 electrical power is generally supplied to the rotating gantry by means of slip ring contacts.

Recorded projection profiles are generally transmitted from the gantry to a computer by means of wireless communication technologies. The design and engineering of the table, as with the gantry, are critical to allowing accurate acquisition of data at high rotational speeds.(Dance et al., 2014)

2.3.2 The X ray tube and generator

Owing to the high X ray flux required for CT, the X ray tube uses a tungsten anode designed to withstand and dissipate high heat loads. With long continuous acquisition cycles, a forced cooling system using oil or water circulated through a heat exchanger is often used.(Dance et al., 2014)

2.3.3. Collimation and filtration

The X ray beam should be collimated to the desired dimensions. the beam width in the longitudinal axis is generally small; therefore, the collimated X ray beam is often referred to as a fan beam. in the plane perpendicular to the table motion, also known as the x–y or axial plane, the beam is shaped to reduce the dynamic range of the signal that is recorded by the detectors. beam shaping(bowtie) filters are used to achieve the desired gradient, with one of a number of mounted bowtie

filters moved into the X ray beam during acquisition.(Dance et al., 2014)

2.3.4. Detectors

The essential physical characteristics of CT detectors are a good detection efficiency and a fast response with little afterglow. currently, solid statedetectors1 are used, as they have a detection efficiency close to 100% compared with high pressure, xenon filled ionization chambers that were used previously and that had a detection efficiency of about 70%. solid state detectors are generally scintillators, meaning that the X rays interacting with the detector generate light. this light is converted to an electrical signal, by photodiodes that are attached to the back of the scintillator, which should have good transparency to ensure optimal detection.

typically, an antiscatter grid is mounted at the front of the detector, which consists of small strips of highly attenuating material (e.g. tungsten) aligned along the longitudinal (z) axis of the CT scanner, forming a 1-D antiscatter grid.

A detector row consists of thousands of dells that are separated by septa designed to prevent light generated in one del from being detected byneighbouringdels. these septa and the strips of the antiscatter grid should be as small as possible since they reduce the effective area of the detector and thus reduce the detection of X rays.(Dance et al., 2014)

2.4. Detector pitch and collimation pitch

Pitch is a parameter that comes to play when helical scan protocols are used. In a helical CT scanner with one detector array, the pitch is determined by the collimator (collimator pitch) and is defined as:

$$Collimator\ pitch = \frac{table\ movement(mm) per\ 360\ rotation\ of\ gantry}{collimator\ width(mm) at\ isocenter} \ldots\ldots\ldots\ldots (1)$$

It is customary in CT to measure the collimator and detector widths at the isocenter of the system. The collimator pitch (Fig.) represents the traditional notion of *pitch,* before the introduction of multiple detector array CT scanners. Pitch is an important component of the scan protocol, and it fundamentally influences radiation dose to the patient, image quality, and scan time. For single detector array scanners, a pitch of 1.0 implies that the number of CT views acquired, when averaged over the long axis of the patient, is comparable to the number acquired with contiguous axial CT. A pitch of less than 1.0 involves over scanning, which may result some slight improvement in image quality and a higher radiation dose to the patient.

CT manufacturers have spent a great deal of developmental effort in optimizing scan protocols for pitches greater than 1.0, and pitches up to 1.5 are commonly used. Pitches with values greater than 1.0 imply some degree of partial scanning along the long axis of the patient. The benefit is faster scan time, less patient motion, and, in some circumstances, use of a smaller volume of contrast agent. Although CT acquisitions around 360 degrees are typical for images of the highest fidelity, the minimum requirement to produce an adequate CT image is a scan of180 degrees plus the fan angle. With fan angles commonly at about 60 degrees, this means that, at a minimum, (180 + 60)/360, or 0.66, of the full circle is required.

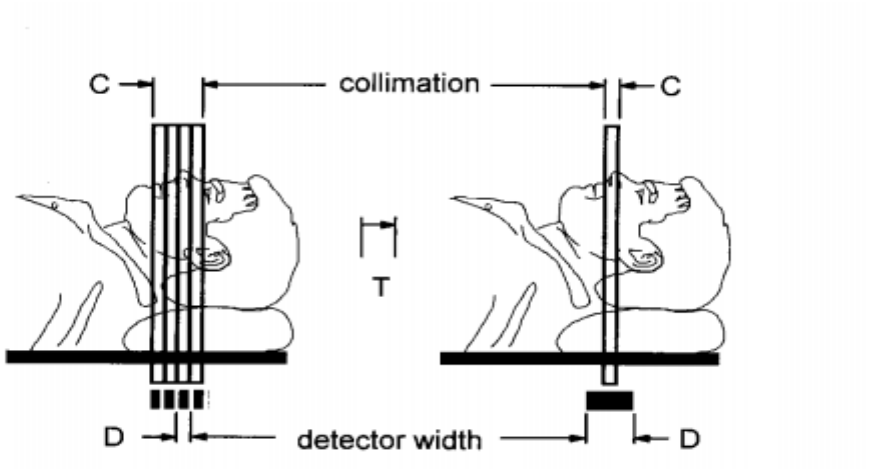

Fig (2.4) *Detector pitch and collimation pitch.*

With a single detector array computed tomographic (CT) scanner, the collimation width is always narrower than the maximum single detector width. A multiple detector array scanner uses collimation that is always wider than a single detector array width. Letting T represent the table translation distance during a360-degree rotation of the gantry, C would be the collimation width and 0 would be the detector width.

Collimator pitch is defined as *T/C,* and detector width is defined by *T/D.* For a multiple detector array CT scanner with four detector arrays, a collimator pitch of 1.0 is equal to a detector pitch of 4.0.

The need to define detector pitch and collimator pitch arises because beam utilization between single and multiple detector array scanners is different. For a multiple detector array scanner with N detector arrays, the collimator pitch is as follows:

$$\text{Collimator pitch} = \frac{\text{Detector pitch}}{\text{N}} \ldots\ldots\ldots\ldots\ldots\ldots\ldots\ldots\ldots (2)$$

For scanners with four detector arrays, detector pitches running from 3 to 6 are used. A detector pitch of 3 for a four-detector array scanner

is equivalent to a collimator pitch of 0.75 (3/4), and a detector pitch of 6 corresponds to a collimator pitch of 1.5 (6/4).(Bushberg et al., 2003)

2.5. Data Acquisition System (DAS)

When the detector generates the analog or electrical signal it is directed to the data acquisition system (DAS). The analog signal generated by the detector is a weak signal and must be amplified to further be analyzed. Amplifying the electrical signal is one of the tasks performed by the data acquisition system (DAS). The DAS is located in the gantry right after or above the detector system. In some modern CT scanning systems, the signal amplification occurs within the detector itself.

Before the projection or raw data, which is currently in the form of an electrical or analog signal, goes to the computer it must be converted to digital information. The computer does not "understand" analog signals therefore, the information must be converted to digital information. This task is accomplished by an analog to digital converter which is an essential component of the DAS. The digital signal is transferred to an array processor.

The array processor solves the statistical information using algorithmic calculations essential for mathematical reconstruction of a CT image. An array processor is a specialized high-speed computer designed to execute mathematical algorithms for the purpose of reconstruction.

The array processor solves reconstruction mathematics faster than a standard microprocessor. It is important to note that special algorithms may require several seconds to several minutes for a standard microprocessor to compute. Recently, processors that compute CT reconstruction mathematics faster than an array processors have been utilized to solve reconstruction mathematics essential to the

development of CT fluoroscopy. The term image or reconstruction generator is used to describe this type of computer.(L.Reddinger, 1997)

2.6. Dosimetric quantities and units

2.6.1. particle fluence($\boldsymbol{\Phi}$)

The particle fluence is the quotient d$N$by dA, where d$N$is the number of particles incident on a sphere of cross-sectional area dA:

$$\Phi = \frac{\mathrm{dN}}{\mathrm{dA}} \ldots\ldots\ldots\ldots\ldots\ldots\ldots\ldots (3)$$

The unit of particle fluence is m–2.

2.6.2. Energy Fluence (ψ)

The energy fluence is the quotient of dE by dA, where dE is the radiant energy incident on a sphere of cross-sectional area dA:

$$\Psi = \frac{\mathrm{dE}}{\mathrm{dA}} \ldots\ldots\ldots\ldots\ldots\ldots\ldots\ldots (4)$$

The unit of energy fluence is J/m2.

2.6.3. Kerma(K)

Kerma is an acronym for kinetic energy released per unit mass. It is a non-stochastic quantity applicable to indirectly ionizing radiations such as photons and neutrons.

It quantifies the average amount of energy transferred from indirectly ionizing radiation to directly ionizing radiation without concern as to what happens after this transfer. The energy of photons is

imparted to matter in a two-stage process. In the first stage, the photon radiation transfers energy to the secondary charged particles (electrons) through various photon interactions (the photoelectric effect, the Compton effect, pair production, etc.). In the second stage, the charged particle transfers energy to the medium through atomic excitations and ionizations.

In this context, the kerma is defined as the mean energy transferred from the indirectly ionizing radiation to charged particles (electrons) in the medium dE_{tr}per unit mass dm:

$$K = \frac{dE_{tr}}{dm} \ldots\ldots\ldots\ldots\ldots\ldots\ldots\ldots\ldots (5)$$

The unit of kerma is joule per kilogram (J/kg). The name for the unit of kerma is the Gray (Gy), where 1 Gy = 1 J/kg.

2.6.4. Absorbed Dose

Absorbed dose is a non-stochastic quantity applicable to both indirectly and directly ionizing radiations. For indirectly ionizing radiations, energy is imparted to matter in a two-step process. In the first step (resulting in kerma), the indirectly ionizing radiation transfers energy as kinetic energy to secondary charged particles.

In the second step, these charged particles transfer some of their kinetic energy to the medium (resulting in absorbed dose) and lose some of their energy in the form of radiative losses (bremsstrahlung, annihilation in flight). The absorbed dose is related to the stochastic quantity energy imparted.

The absorbed dose is defined as the mean energy imparted by ionizing radiation to matter of mass m in a finite volume V by:

$$D = \frac{d\varepsilon}{dm} \ldots\ldots\ldots\ldots\ldots\ldots\ldots\ldots (6)$$

The energy imparted ε is the sum of all the energy entering the volume of interest minus all the energy leaving the volume, taking into account any mass–energy conversion within the volume. Pair production, for example, decreases the energy by 1.022 MeV, while electron–positron annihilation increases the energy by the same amount. That because electrons travel in the medium and deposit energy along their tracks, this absorption of energy does not take place at the same location as the transfer of energy described by kerma.

The unit of absorbed dose is joule per kilogram (J/kg). The name for the unit of absorbed dose is the gray (Gy).(Podgorsak, 2005)

2.7. Quantities for CT Dosimetry

2.7.1. Computed Tomography Dose Index (CTDI)

The CTDI is the primary dose measurement concept in CT

$$CTDI = \frac{1}{NT} \int_{-\infty}^{\infty} D(z)dz \ldots\ldots\ldots\ldots\ldots\ldots\ldots\ldots\ldots (7)$$

Where:

D(*z*) = the radiation dose profile along the z-axis, *N* = the number of tomographic sections imaged in a single axial scan. This is equal to the number of data channels used in a particular scan. The value of *N* may be less than or equal to the maximum number of data channels available on the system.

T = the width of the tomographic section along the z-axis imaged by one data channel. In multiple-detector-row (multi slice) CT scanners,

several detector elements maybe grouped together to form one data channel. In single-detector-row (single-slice) CT, the z-axis collimation (T) is the nominal scan width. CTDI represents the average absorbed dose, along the z-axis, from a series of contiguous irradiations. It is measured from one axial CT scan (one rotation of the x-ray tube) and is calculated by dividing the integrated absorbed dose by the nominal total beam collimation. The CTDI is always measured in the axial scan mode for a single rotation of the x-ray source, and theoretically estimates the average dose within the central region of a scan volume consisting of multiple, contiguous CT scans [Multiple Scan Average Dose (MSAD)] for the case where the scan length is sufficient for the central dose to approach its asymptotic upper limit.

The MSAD represents the average dose over a small interval (-I/2, I/2) about the center of the scan length ($z = 0$) for a scan interval I, but requires multiple exposures for its direct measurement. The CTDI offered a more convenient yet nominally equivalent method of estimating this value, and required only a single-scan acquisition, which in the early days of CT, saved a considerable amount of time.(McCollough et al., 2008a)

2.7.2. $CTDI_{FDA}$

Theoretically, the equivalence of the MSAD and the CTDI requires that all contributions from the tails of the radiation dose profile be included in the CTDI dose measurement. The exact integration limits required to meet this criterion depend upon the width of the nominal radiation beam and the scattering medium. To standardize CTDI measurements (infinity is not a likely measurement parameter), the FDA introduced the integration limits of ±7T, where T represented the nominal slice width.

Interestingly, the original CT scanner, the EMI Mark I, was a dual detector-row system. Hence, the nominal radiation beam width was equal to twice the nominal slice width (i.e., N *x* T mm). To account for this, the CTDI value must be normalized to 1/NT:

$$CTDI_{FAD} = \frac{1}{NT} \int_{-7T}^{7T} D(z)dz \ldots\ldots\ldots\ldots\ldots\ldots\ldots\ldots\ldots (8)$$

2.7.3. $CTDI_{100}$

CTD_{100} represents the accumulated multiple scan dose at the center of a 100-mm scan and underestimates the accumulated dose for longer Scan lengths.

It is thus smaller than the equilibrium dose or the MSAD. The $CTDI_{100}$, like the $CTDI_{FAD}$ requires integration of the radiation dose profile from single axial scan over specific integration limits.

In the case of $CTDI_{100}$, the integration limits are ±50 mm, which corresponds to the 100-mm length of the commercially available "pencil" ionization chamber as described in equation below:

$$CTDI_{100} = \frac{1}{NT} \int_{-50}^{50} D(z)dz \ldots\ldots\ldots\ldots\ldots (9)$$

2.7.4. Weighted $CTDL_W$

The CTDI varies across the field of view (FOV). For example, for body CT imaging, the CTDI is typically a factor or two higher at the surface than at the center of the FOV. The average CTDI across the FOV is estimated by the Weighted CTDI ($CTDI_W$),

Where:

$$CTDI_W = {}^1\!/_3\, CTDI_{100,center} + {}^2\!/_3\, CTDI_{100,edge} \ldots\ldots\ldots (10)$$

The values of 1/3 and 2/3 approximate the relative areas represented by the center and edgevalues31. CTDIw is a useful indicator of scanner radiation output for a specific Kvp and mAs.(McCollough et al., 2008a)

2.7.5. Volume $CTDI_{VOL}$

To represent dose for a specific scan protocol, which almost always involves series of scans, it is essential to take into account any gaps or overlaps between the x-ray beams from consecutive rotations of the X-ray source. This is accomplished with use of a dose descriptor known as the Volume $CTDI_W$ ($CTDI_{VOL}$),

Where:

$$CTDI_{VOL} = \frac{NT}{I} \times CTDI_W \ldots\ldots\ldots (11)$$

Where: I = the table increment per axial scan (mm) Since the pitch is defining as the ratio of the table travel per rotation (I) to the total nominal beam width (N×T).

$$pitch = \frac{I}{NT} \ldots\ldots\ldots\ldots\ldots\ldots\ldots\ldots\ldots (12)$$

Thus, the volume CTDI can expressed as:

$$CTDI_{vol} = \frac{1}{pitch} \times CTDI_W \ldots\ldots\ldots\ldots (13)$$

Whereas $CTDI_W$ represents the average absorbed radiation dose over the *x* and *y* directions at the center of the scan from a series of axial scans where the scatter tails are negligible beyond the 100-mm integration limit, $CTDI_{vol}$represents the average absorbed radiation dose over the *x*, *y*, and *z* directions. The $CTDI_{vol}$ provides a single CT

dose parameter, based on a directly and easily measured quantity, which represents the average dose within the scan volume for a standardized (CTDI) phantom. The SI units are milligram (mGy). CTDIvol is a useful indicator of the dose to a standardized phantom for a specific exam protocol, because it takes into account protocol-specific information such as pitch. Its value may be displayed prospectively on the console of newer CT scanners, although it may be mislabeled on some systems as CTDIw.(McCollough et al., 2008a)

2.7.6. Dose Length Product (DLP)

To better represent the overall energy delivered by a given scan protocol, the absorbed dose can be integrated along the scan length to compute the Dose-Length Product (DLP), where

$$\text{DLP}\ (\text{mGy} - \text{cm}) = \text{CTDIvol x scan length}\ (\text{cm}) \ldots\ldots\ldots (14)$$

The DLP reflects the total energy absorbed (and thus the potential biological effect) attributable to the complete scan acquisition.

Thus, an abdomen-only CT exam might have the same CTDIvol as an abdomen/pelvis CT exam, but the latter exam would have a greater DLP, proportional to the greater z-extent of the scan volume.

In helical CT, data interpolation between two points must be performed for all projection angles. Thus, the images at the very beginning and end of a helical scan require data from z-axis projections beyond the defined "scan" boundaries (i.e., the beginning and end of the anatomic range over which images are desired). This increase in DLP due to the additional rotation(s) required for the helical interpolation algorithm is often referred to as "over ranging." For MDCT scanners, the number of additional rotations is strongly pitch dependent, with a typical increase in irradiation length of 1.5 times the total nominal beam width. The

implications of over ranging with regard to the DLP depends on the length of the imaged body region. For helical scans that are short relative to the total beam width, the dose efficiency (with regard to over ranging) will decrease.

For the same anatomic coverage, it is generally more dose efficient to use a single helical scan than multiple helical scans.(McCollough et al., 2008a)

2.8. System of Radiological Protection

In the 1990 Recommendations, the Commission gave principles of protection for exercise separately from interference status. The Commission continues to regard these principles as fundamental for the system of protection, and has now formulated a single set of principles that apply to planned, emergency, and existing exposure situations.

In these Recommendations, the Commission also clarifies how the fundamental principles apply to radiation sources and to the individual, as well as how the source-related principles apply to all controllable situations. (Valentin, 2007)

2.8.1. Justification:

No practice or source within practice should be authorized unless it produces sufficient benefits to the exposed individuals or society, to offset the radiation harm that it might cause. That is unless the practice is justified, taking into account social, economic and other relevant face. (Rehani et al., 2010)

2.8.2. Optimization:

In relation to exposure from any particular source within practice, protection and safety shall be optimized in order to keep the magnitude of individual doses, the number of people exposed, and the likelihood

of incurring exposures as low as reasonably achievable. Economic and social factors being taken into account, within the restriction that the doses to individuals delivered by the source shall be subjected to dose constraints. (Rehani et al., 2010)

2.8.3. Dose limitation:

The normal exposure of individuals shall be restricted so that neither the total effective dose nor the total equivalent dose to relevant organs or tissues, caused by the possible combination of exposures from authorized practices, the limit on effective dose represents the level above which the risk of stochastic effects due to radiation is considered to be unacceptable.

For localized exposure of the lens of the eye, extremities and the skin, this limit on effective dose is not sufficient to ensure the avoidance of deterministic effects, and therefore limits on equivalent dose are specified for such situations. (Valentin, 2007)

2.9. Radiation Quantities

The absorbed dose is the basic physical dosimetry quantity, but it is not entirely satisfactory for radiation protection purposes because the effectiveness in damaging human tissue differs for different types of ionizing radiation. In addition to the physical quantities, other dose related quantities have been introduced to account not only for the physical effects but also for the biological effects of radiation upon tissues. These quantities are organ dose, equivalent dose, effective dose, committed dose and collective dose.(Podgorsak, 2005)

2.9.1. Organ dose

Organ dose $D_T$is defined as mean dose in a specified tissue or organ T of the human body, given by:

$$D_T = \frac{\varepsilon_T}{m_T} \ldots\ldots\ldots\ldots\ldots\ldots\ldots\ldots (15)$$

Where:

- m_T is the mass of the organ or tissue under consideration.
- ε_T is the total energy imparted by radiation to that tissue or organ.

2.9.2. Equivalent Dose

The biological detriment (harm) to an organ depends not only on the physical average dose received by the organ but also on the pattern of the dose distribution that results from the radiation type and energy. For the same dose to the organ, or neutron radiation will cause greater harm compared with gamma rays or electrons.

This is because the ionization events produced by a neutron radiation will be much more closely spaced (densely ionizing radiations) and so there is a higher probability of irreversible damage to the chromosomes and less chance of tissue repair. Consequently, the organ dose is multiplied by a radiation weighting factor W_R to account for the effectiveness of the given radiation in inducing health effects; the resulting quantity is called the equivalent dose H_T.The equivalent dose H_T is defined as:

$$H_T = D \times W_R \ldots\ldots\ldots\ldots\ldots\ldots\ldots\ldots (16)$$

Where D is the absorbed dose and W_R is the radiation weighting factor.

The SI unit of equivalent dose is J/kg and its name is the Sievert (Sv) The organ dose is a measure of the energy absorption per unit mass averaged over the organ, while the equivalent dose is a measure of the consequent biological harm (detriment) to the organ or tissue.(Podgorsak, 2005)

Table. (2.1): Radiation weighting factors in publication ICRP 60 and Q in publication ICRP 60:

Type and energy range	W_T	Q
Photons (x-ray and gamma rays) all energies	1	1
Electron, muons, all energies	1	1
Neutrons < 10 KeV	5	-
Neutrons 10 keV to 100 keV	10	-
Neutrons > 100 KeV to 2MeV	20	-
Neutrons > 2 MeV to 20 MeV	10	-
Neutrons > 20 MeV	5	-
Protons > 20 MeV	5	1
Alpha particles fission- fragment heavy nuclei	20	20

2.9.3. Effective dose

The effective dose E is defined as the summation of tissue equivalent doses, each multiplied by the appropriate tissue weighting factor W_T, to indicate the combination of different doses to several different tissues in a way that correlates well with all stochastic effects combined.

$$E = \sum W_T \times H_T \dots\dots\dots\dots\dots\dots\dots\dots\dots (17)$$

The unit of the quantity is the sievert (Sv), which is 1 J kg^{-1}. A commonly used subunit is the millisievert (mSv) or one-thousandth of a Sv.(Kainz, 2006)

Table (2.2): Tissue weighting factors for different organs.

Organs	Tissue weighting factors		
	ICRP30(1979)	ICRP60(1990)	ICRP103(2007)
Gonads	0.25	0.20	0.08
Clon	-	0.12	0.12
Lung	0.12	0.12	0.12
Red bone marrow	0.12	0.12	0.12
Stomach	-	0.12	0.12
Bladder	-	0.05	0.04
Breast	0.15	0.05	0.12
Liver	-	0.05	0.04
Esophagus	-	0.05	0.04
Thyroid	0.03	0.05	0.04
Bone surface	0.03	0.01	0.01
Skin	-	0.01	0.01
Brain	-	-	0.01
Salivary	-	-	0.01
Remained	0.03	0.05	0.01

(Protection, 2007)

2.9.3.1 Effective Dose (E) in CT

It is important to recognize that the potential biological effects from radiation depend not only on the radiation dose to a tissue or organ, but also on the biological sensitivity of the tissue or organ irradiated. Effective dose, E, is a dose descriptor that reflects this difference in biologic sensitivity. It is a single dose parameter that reflects the risk of a non-uniform exposure in terms of an equivalent whole-body exposure.

The units of effective dose are Sievert (usually millisieverts (mSv) are used in diagnostic radiology). The concept of effective dose was designed for radiation protection of occupationally exposed personnel. It reflects radiation detriment averaged over gender and age, and its application has limitations when applied to medical populations. However, it does facilitate the comparison of biologic effect between diagnostic exams of different types. The use of effective dose facilitates communication with patients regarding the potential harm of a medical exam that uses ionizing radiation.

It is important to remember, however, that the effective dose describes the relative "whole body" dose for a particular exam and scanner, but is not the dose for any one individual. Effective dose calculations use many assumptions, including a mathematical model of a "standard" human body that does not accurately reflect any one individual (it is and erogenous and of an age representative of a radiation worker). Effective dose is best used to optimize exams and to compare risks between proposed exams. It is a broad measure of risk, and as such, should not be quoted with more than one or two significant digits. The most direct way of estimating doses to patients undergoing CT examinations is to measure organ doses in patient-like phantoms. Another way of obtaining the pattern of energy deposition in patients undergoing CT examinations is by calculation.(McCollough et al., 2008b)

Computations that use Monte Carlo methods follow the paths of a large number of x-rays as they interact with a virtual phantom and estimate the probability of the dominant interaction processes (i.e., Compton scatter and photo electric absorption). This type of calculation assumes that the patient resembles the phantom used for measurements or Monte Carlo simulation. When patients differ in size and composition,

appropriate corrections might need to be used. The resultant information is the absorbed dose to a specified tissue, which may be used to predict the biological consequences to that (single) tissue. CT examinations, however, irradiate multiple tissues having different radiation sensitivities. The effective dose takes in to account how much radiation is received by an individual tissue, as well as the tissue's relative radiation sensitivity. Specific values of effective dose can be calculated using several different software packages, which are based on the use of data from one of two sources, the National Radiological Protection Board (NRPB) in the United Kingdom or the Institute of Radiation Protection (GSF) in Germany.(McCollough et al., 2008b)

A free Excel spreadsheet can be downloaded from organ dose and effective dose estimates using the NRPB organ dose coefficients. Other packages are available for purchase. The European Working Group for Guidelines on Quality Criteria in Computed Tomography was also proposed a generic estimation method to minimize controversy in calculation different effective dose. Effective dose values calculated from the NRPB Monte Carlo organ coefficients were compared to DLP values for the corresponding clinical exams to determine a set of coefficients k, where the values of k are dependent only on the region of the body being scanned (head, neck, thorax, abdomen, or pelvis).

Using this methodology, E can be estimated from the DLP, which is reported on most CT systems: The values of E predicted by DLP and the values of E estimated using more rigorous calculations methods are remarkably consistent, with a maximum deviation from the mean of approximately10% to 15%. Hence, the use of DLP to estimate E appears to be a reasonably robust method for estimating effective dose**.**(McCollough et al., 2008b)

2.10. Literature review

OSMAN, NAIF MOHAMMED (2016) was reported of Assessment of Radiation Dose for Patients Undergoing Brain and Abdomen Computed Tomography. Were a total of 128 adult patients undergoing brain and the abdominal CT scanning exams were evaluated using CT Dose index and dose length product (DLP) Were the result revealed that the mean effective dose for abdomen in hospital (1) and hospital (2) was (64.31 ± 29.8) mSv and (71.61 ± 0.97) mSv respectively. The mean effective dose for brain in hospital (1) and hospital (2) was (2.96 ± 0.97) mSv, (3.11±0.51) mSv respectively. These values were found to be at standard dose reference level. Unjustified screening the Abdomen and head should thus be banished. Such policy is unacceptable in young patients who are at a low risk of having an incidental associated disease. Similarity, repeated acquisition should not be performed in circumstances where they do not specifically yield additional information.(OSMAN, 2016)

Ulla Nikupaavo et al (2015), reported the evaluation lens dose in Routine Head CT: Comparison of Different Optimization Methods with Anthropomorphic Phantoms. Were used Two anthropomorphic phantoms were scanned with routine head CT protocol for evaluation of the brain that included bismuth shielding, gantry tilting, organ-based tube current modulation, or combinations of these techniques.

High sensitivity metal oxide semiconductor field effect transistor dosimeters were used to measure local equivalent doses in the head region. The relative changes in image noise and contrast were determined by ROI analysis. The mean absorbed lens doses varied from 4.9 to 19.7 mGy and from 10.8 to16.9 mGy in the two phantoms.

The most efficient method for reducing lens dose was gantry tilting, which left the lenses outside the primary radiation beam, resulting in an approximately75% decrease in lens dose. Image noise decreased, especially in the anterior part of the brain.

The use of organ-based tube current modulation resulted in an approximately 30% decrease in lens dose. However, image noise increased as much as 30% in the posterior and central parts of the brain. With bismuth shields, it was possible to reduce lens dose as much as 25%. Our results indicate that gantry tilt, when possible, is an effective method for reducing exposure of the eye lenses in CT of the brain without compromising image quality. Measurements in two different phantoms showed how patient geometry affects the optimization. When lenses can only partially be cropped outside the primary beam, organ-based tube current modulation or bismuth shields can be useful in lens dose reduction. (Nikupaavo et al., 2015)

N.N. Jibiri et al, (2014) reported of Estimation of radiation dose to the lens of eyes of patients undergoing cranial computed tomography in a teaching Hospital in Osun state, Nigeria, were the Entrance Surface Dose (ESD) to the lens of eyes of 26 patients who had cranial CT procedures at a University Teaching Hospital in Ile-Ife, Nigeria has been determined in order to assess the level of radiation protection compliance and optimization of radiation safety at the hospital. The Results indicate that the doses to the patients ranged between 17.13mGy and 51.98 mGy within the period under study.

The average doses obtained for the pediatric patients (1.5-18 yrs.), young adults (19-49 yrs.) and adults (≥50 yrs.) were 31.14 ±11.02 mGy, 41.81±12.60 mGy and 31.97 ± 11.31mGy respectively.

The mean dose obtained in this study was lower than threshold for lens damage, therefore the dose recorded in this study is clinically safe. This study represents a requisite pedestal on the need for a nation-wide evaluation and investigation of optimization of procedures in radiological examinations with a view to establishing a national dosimetry protocol and reference dose level or guidance level in the country.(Jibiri and Adewale, 2014)

Hassan, Omer Ahmed Mahgoub (2012) was reported of Estimation of Patient's Effective Dose during Routine Computed Tomography Examinations Computed tomography (CT), is an X-ray procedure that generates high quality cross-sectional images of the body, and by comparison to other radiological diagnosis, CT is responsible for higher doses to patients. The radiation dose was measured in five hospitals in Khartoum state during (March 2012- July 2012) using different CT modalities. The radiation dose higher Al-amal, Royal scan and Al- zaytouna hospital than the other two hospitals while the radiation dose in Al-bugaa diagnostic center and Al-ribat university hospital the lowest. MSCT scanners 64 slice exposed patients to a higher dose than 16 slice scanners. In this study, the mean effective dose for Al-Zaytouna hospital was 4.3±1.7 mSv, 20.5±6.6mSv and 62.3±32.5 mSv for the brain, chest and abdomen respectively. The mean effective dose for Royal scan hospital was 3.8±1.4 mSv, 28.1±36.5 mSv, 46.2±34.2 mSv for brain, chest and abdomen respectively. The mean effective doses for Al Bugaa diagnostic center were 2.7±1.4 mSv, 8.5±3.4 mSv, 18.2±13.1 mSv for brain, chest and abdomen respectively. The mean effective dose for Al amal diagnostic center was 3.2±1.6 mSv, 12.5±9.7 mSv, 36.9±20.6 mSv for brain, chest and abdomen respectively.

The mean effective dose for Al Ribat university hospital was 1.6±0.9 mSv, 3.2±1.8 mSv, 8.7±5.7 mSv for brain, chest and abdomen respectively and the effective dose is median than that reported in previous studies.(Hassan, 2012)

S. Suzuki et al, (2010) reported of Lens Exposure during Brain Scans Using Multi detector Row CT Scanners. With 8 types of multi detector row CT scanners, both axial and helical scans were obtained for the head part of a human-shaped phantom by using normal clinical settings with the orbit meatal line as the baseline. We measured the doses on both eyelids by using an RPLGD during whole-brain scans including the orbit with the starting point at the level of the inferior orbital rim.

To assess the effect of the starting points on the lens doses, we measured the lens doses by using 2 other starting points for scanning (the orbit meatal line and the superior orbital rim). The CTDIvol and the lens doses during whole-brain CT including the orbit were 50.9–113.3mGy and 42.6–103.5 mGy, respectively. The ratios of lens dose to CTDIvol were 80.6%–103.4%. The lens doses decreased as the starting points were set more superiorly. The lens doses during scans from the superior orbital rim were 11.8%–20.9% of the doses during the scans from the inferior orbitalrim. CTDIvol can be used to estimate the lens dose during whole-brain CT when the orbit is included in the scanning range.(Suzuki et al., 2010)

J.S.P. Tan et al (2009) was reported of Comparison of Eye Lens Dose on Neuroimaging Protocols between 16- and 64-Section Multi detector CT Achieving the Lowest Possible Dose, the aim was to assess radiation-dose differences between 16- and 64-section MDCT from the same manufacturer, by using near-identical neuroimaging protocols,

were Three cadaveric heads were scanned on 16- and 64-section MDCT by using standard neuroimaging CT protocols. Eye lens dose was measured by using thermoluminescent dosimeters (TLD), and each scanning was repeated to reduce random error.

The dose-length product, volume CT dose index (CTDIvol), and TLD readings for each imaging protocol were averaged and compared between scanners and protocols, by using the paired Student t test. Statistical significance was defined at P› .05. were the radiation dose delivered and eye lens doses were lower by 28.1%–45.7% (P› .000) on the 64-section MDCT for near-identical imaging protocols. On the 16-section MDCT, lens dose reduction was greatest (81.1%) on a tilted axial mode, compared with a nontilted helical mode for CT brain scans. Among the protocols studied, CT of the temporal bone delivered the greatest radiation dose to the eye lens.

Eye lens radiation doses delivered by the 64-section MDCT are significantly lower, partly due to improvements in automatic tube current modulation technology. However, where applicable, protection of the eyes from the radiation beam by either repositioning the head or tilting the gantry remains the best way to reduce eye lens dose.(Tan et al., 2009)

Justin E et al, (2006) reported of Estimation of patient organ doses from CT examinations in Tanzania. The aims of this study are, first, to determine the magnitude of radiation doses received by selected radiosensitive organs of patients undergoing CT examinations and compare them with other studies, and second, to assess how CT scanning protocols in practice affect patient organ doses. In order to achieve these objectives, patient organ doses from five common CT examinations were obtained from eight hospitals in Tanzania.

The patient organ doses were estimated using measurements of CT dose indexes (CTDI), exposure-related parameters, and the ImPACT spreadsheet based on NRPB conversion factors. A large variation of mean organ doses among hospitals was observed for similar CT examinations. These variations largely originated from different CT scanning protocols used in different hospitals and scanner type.

The mean organ doses in this study for the eye lens (for head), thyroid (for chest), breast (for chest), stomach (for abdomen), and ovary (for pelvis) were 63.9 mGy, 12.3 mGy, 26.1 mGy, 35.6 mGy, and 24.0 mGy, respectively. These values were mostly comparable to and slightly higher than the values of organ doses reported from the literature for the United Kingdom, Japan, Germany, Norway, and the Netherlands. It was concluded that patient organ doses could be substantially minimized through careful selection of scanning parameters based on clinical indications of study, patient size, and body region being examined. Additional dose reduction to superficial organs would require the use of shielding materials.(Ngaile and Msaki, 2006)

Marc K et al, (2005) reported of evaluation radiation doses to the eye and parotids during CT of the sinuses, nine cadaver heads were scanned in the axial plane by means of a fine-cut (0.75 mm) protocol. Images were then reconstructed in the coronal and sagittal planes for use with the image guidance software. Thermoluminescent dosimeters were taped over the eyes and parotids and used to measure the radiation dose absorbed by these organs. Were doses obtained were 29.5 mGy for the lens and around 30 mGy for the parotid**.** The measured doses are lower than the reported acute thresholds of 500-2000 mGy for lens opacities and well below the threshold of 2500 mGy for damage to the parotid.

These results demonstrate minimal risk from radiation through the use of high-resolution computed tomography and support the use of such a protocol for diagnosis and preoperative planning.(Bassim et al., 2005)

CHAPTER THREE

MATERIALS & METHODS

Chapter Three

Materials & Method

3.1. Materials

3.1.1 Machines:

The CT scanners used in this study were (CT Toshiba 64 slice) and (CT Toshiba 16 slice).

3.1.2 Population:

The population in this study were 117 adult patients underwent brain CT scan in four hospitals in Khartoum state during April to August 2018.

3.2 Methods

3.2.1 Data Collection:

The data were collected using a sheet for all patients in order to maintain consistency of the information from display.

A data collected sheet was designed to evaluate the patient doses, the collected data included demographic information (sex and age), scan parameters (KV, mAs, slice thickness, scan time, number of slice, and scan length), and dosimetric information (CTDI, and DLP).

3.2.2. Dosimetric calculations

CT Expo software was used to calculate common CT dose descriptors: (i) CT weighted dose index ($CTDI_W$), (ii) volume dose index ($CTDI_{vol}$) provides an indication of the average absorbed dose in the scanned region, (iii) CT dose –length product (DLP) the integrated absorbed dose along a line parallel to the axis of rotation for the complete CT examination, (vi) effective dose (E): a method for comparing patient doses from different diagnostic procedures (Effective dose) and (iiv) organ dose.

3.2.2.1 CT-Expo V 2.5 software

The CT-Expo Version 2.5 software tool used for dose calculations and CT-Expo tools—based on Monte Carlo data published by the Research Center for Environment and Health in Germany—for dose calculation.

Dose estimation is done based on mathematical phantoms for adult (ADAM and EVA).

3.2.3 Data Analysis

The data in this study were analysis by using Microsoft Excel and SPSS software**.**

CHAPTER FOUR

RESULTS

Chapter Four

Results

4.1. Results:

The results of this study are presented for dose measurements performed in four CT units, two CT scanner Toshiba model Acquilion (64-slice) versus two CT scanner Toshiba model Acquilion (16-slice), and 120 CT examinations in patients, doses were estimated in terms of $CTDI_{vol}$, DLP and E, the tables below describe the results in detail.

Table (4.1) summaries the characteristic statistics parameters for the hospital (A) from The CT scanner Toshiba model Acquilion 64-slice:

(Kv: 120, mAs:225 and Pitch: 0.5 for all patients in this center)

	Mean	**Median**	**STD**	**Min**	**Max**	**3d Quartile**
Age	61.40	70	23.93	22	95	85.00
CTDI	79.200	79.200	0.000	79.2	79.2	79.200
DLP	1502.926	1500.286	111.4896	1302.286	1777.486	1539.886
E	4.610	4.500	0.9308	3.2	8.0	5.000

Table (4.2) summaries the characteristic statistics parameters for the hospital (A) from The CT scanner Toshiba model Acquilion (64-slice), for male:

	Mean	**Median**	**STD**	**Min**	**Max**	**3d Quartile**
Age	68.40	78.00	22.928	28	95	87.00
CTDI	79.200	79.200	0.000	79.2	79.2	79.200
DLP	1502.926	1539.886	130.024	1302.286	1777.486	1539.886
E	4.353	4.400	0.8831	3.2	6.7	4.400

Table (4.3) summaries the characteristic statistics parameters for the hospital (A) from The CT scanner Toshiba model Acquilion (64-slice), for female:

	Mean	**Median**	**STD**	**Min**	**Max**	**3d Quartile**
Age	54.40	47.00	23.576	22	85	84.00
CTDI	79.200	79.200	0.000	79.2	79.2	79.200
DLP	1502.926	1460.686	94.029	1381.486	1777.486	1539.886
E	4.867	4.500	0.935	4.0	8.0	5.000

Table (4.4) the comparison of (E) between male and female from Toshiba CT scanner model Acquilion (64-slice) for the hospital (A):

	Sex		**Total**
E	**Female**	**Male**	
3.2	0	1	1
3.7	0	4	4
4.0	2	2	4
4.4	0	5	5
4.5	6	0	6
4.9	0	1	1
5.0	6	0	6
5.7	0	1	1
6.7	0	1	1
8.0	1	0	1
Total	15	15	30

Table (4.5) summaries the characteristic statistics parameters for the hospital (B) from The CT scanner Toshiba model Acquilion 64-slice (Kv: 120, mAs:225 and Pitch: 0.5 for all patients in this center**)**

	Mean	**Median**	**STD**	**Min**	**Max**	**3d Quartile**
Age	55.70	50.00	25.704	20	95	84.25
CTDI	79.200	79.00	0.0000	79.2	79.2	79.200
DLP	1518.766	1539.886	121.159	1381.486	1777.486	1559.686
E	4.640	4.400	0.856	3.7	6.7	5.000

Table (4.6) summaries the characteristic statistics parameters for the hospital (B) from The CT scanner Toshiba model Acquilion (64-slice) for male:

	Mean	**Median**	**STD**	**Min**	**Max**	**3d Quartile**
Age	53.33	50.00	26.223	20	88	84.25
CTDI	79.200	79.200	.0000	79.2	79.2	79.200
DLP	1553.086	1539.886	130.987	1381.486	1777.486	1619.086
E	4.689	4.400	1.007	3.7	6.7	4.900

Table (4.7) summaries the characteristic statistics parameters for the hospital (B) from The CT scanner Toshiba model Acquilion (64-slice) for female:

	Mean	**Median**	**STD**	**Min**	**Max**	**3d Quartile**
Age	59.25	56.00	25.616	29	95	84.75
CTDI	79.200	79.200	0.0000	79.2	79.2	79.200
DLP	1467.286	1460.686	85.823	1381.486	1619.086	1539.886
E	4.567	4.500	0.5944	4.0	5.8	5.000

Table (4.8) the comparison of (E) between male and female from Toshiba CT scanner model Acquilion (64-slice) for the hospital (B):

E	**Sex**		**Total**
	Female	**Male**	
3.7	0	4	4
4.0	5	1	6
4.4	0	7	7
4.5	2	0	2
4.9	0	3	3
5.0	4	0	4
5.8	1	0	1
6.7	0	3	3
Total	12	18	30

Table (4.9) summaries the characteristic statistics parameters for the hospital (C) from The CT scanner Toshiba model Acquilion 16-slice (Kv: 120, mAs:150 and Pitch: 0.9 for all patients in this center)

	Mean	**Median**	**STD**	**Min**	**Max**	**3d Quartile**
Age	49.89	50.00	18.785	22	84	65.00
CTDI	50.900	50.900	0.0000	50.9	50.9	50.900
DLP	932.799	934.684	105.182	781.942	1240.170	985.599
E	2.830	2.900	0.8236	1.9	5.9	3.100

Table (4.10) summaries the characteristic statistics parameters for the hospital (C) from The CT scanner Toshiba model Acquilion (16-slice) for male:

	Mean	**Median**	**STD**	**Min**	**Max**	**3d Quartile**
Age	53.56	62.00	24.951	22	84	77.50
CTDI	50.900	50.900	.0000	50.9	50.9	50.900
DLP	951.656	934.684	84.432	832.856	1087.427	1011.056
E	2.722	2.800	0.5263	2.0	3.7	3.000

Table (4.11) summaries the characteristic statistics parameters for the hospital (C) from The CT scanner Toshiba model Acquilion (16-slice) for female:

	Mean	**Median**	**STD**	**Min**	**Max**	**3d Quartile**
Age	48.06	50.00	15.364	23	65	63.50
CTDI	50.900	50.900	0.0000	50.9	50.9	50.900
DLP	923.370	934.684	115.2529	781.9416	1240.1702	985.5987
E	2.883	2.900	0.9476	1.9	5.9	3.200

Table (4.12) the comparison of (E) between male and female from Toshiba CT scanner model Acquilion (16-slice) for the hospital (C):

E	**Sex**		**Total**
	Female	**Male**	
1.9	4	0	4
2.0	0	2	2
2.2	1	0	1
2.5	2	0	2
2.6	0	2	2
2.8	0	2	2
2.9	6	1	7
3.1	0	1	1
3.2	2	0	2
3.7	2	1	3
5.9	1	0	1
Total	**18**	**9**	**27**

Table (4.13) summaries the characteristic statistics parameters for the hospital (D) from The CT scanner Toshiba model Acquilion 16-slice ***(***Kv: 120, mAs:150 and Pitch: 0.5 for all patients in this center)

	Mean	**Median**	**STD**	**Min**	**Max**	**3d Quartile**
Age	50.67	57.00	21.157	16	85	67.75
CTDI	61.100	61.100	0.0000	61.1	61.1	61.100
DLP	1138.566	1148.748	55.774	1026.554	1209.846	1164.023
E	3.260	3.200	0.3654	2.5	4.0	3.500

Table (4.14) summaries the characteristic statistics parameters for the hospital (D) from The CT scanner Toshiba model Acquilion (16-slice) for male:

	Mean	**Median**	**STD**	**Min**	**Max**	**3d Quartile**
Age	54.24	60.00	21.839	16	85	72.50
CTDI	61.100	61.100	0.0000	61.1	61.1	61.100
DLP	1141.5605	1148.748	56.669	1026.554	1209.846	1179.297
E	3.129	3.200	0.2779	2.5	3.4	3.300

Table (4.15) summaries the characteristic statistics parameters for the hospital (D) from The CT scanner Toshiba model Acquilion (16-slice) for female:

	Mean	**Median**	**STD**	**Min**	**Max**	**3d Quartile**
Age	46.00	40.00	20.104	17	75	64.50
CTDI	61.100	61.100	0.0000	61.1	61.1	61.100
DLP	1134.649	1148.748	56.625	1026.554	1209.846	1179.297
E	3.431	3.500	0.4049	2.7	4.0	3.750

Table (4.16) the comparison of (E) between male and female from Toshiba CT scanner model Acquilion (16-slice) for the hospital (D):

E	**Sex**		**Total**
	Female	Male	
2.5	0	2	2
2.7	1	0	1
2.9	0	2	2
3.1	4	0	4
3.2	0	9	9
3.4	0	4	4
3.5	5	0	5
4.0	3	0	3
Total	**13**	**17**	**30**

Fieger (4.1) Compare the effective dose between the four centers:

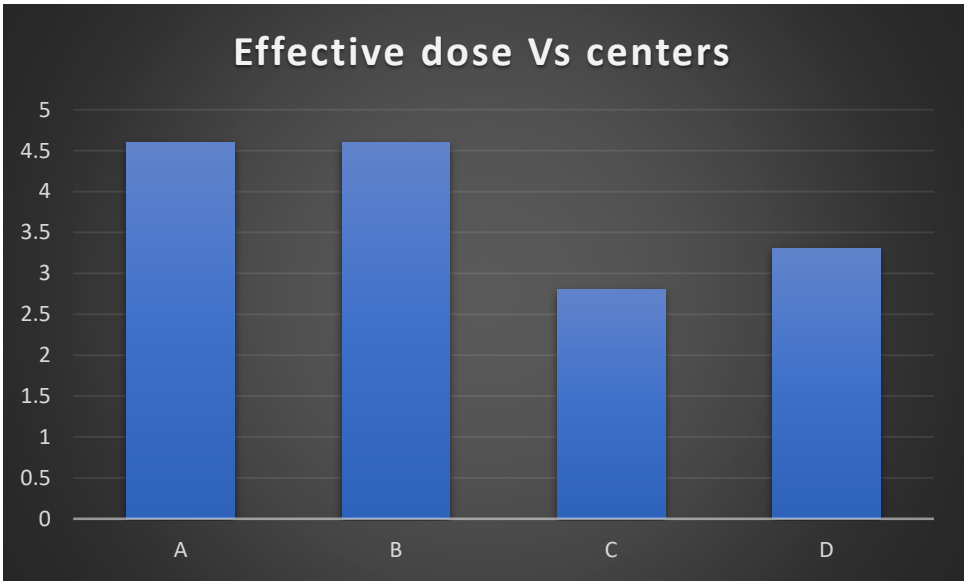

Table (4.17) show the mean of CTDI, DLP and E in this study and compare with other country and EC reference dose:

	This study 2018	Khartoum 2012	Tanzania 2005	Taiwan 2005	UK 2005	EC
$CTDI_{vol}$	67.4	-	43	55	55 - 65	60
DLP	1273.3	-	913	665	700 - 930	1050
E	3.8	3.5	2.1	1.6	2.4	2.4

Table (4.18) showed the organ dose estimated from The CT scanner Toshiba model Acquilion (64-slice) by CT Expo 2.5 software during this study:

	Mean	Median	STD	Min	Max	3d Quartile
Brain	65.753	65.950	1.5556	63.3	67.9	67.175
Salivary gland	74.933	78.250	8.1290	47.9	86.4	80.525
Thyroid	17.420	13.000	14.4126	5.0	73.7	21.100
Esophagus	0.580	0.600	.2469	0.2	1.4	0.700
Lungs	0.437	0.400	0.1752	0.2	1.1	0.500
Bone marrow	9.823	9.900	0.4854	8.8	11.1	10.200
Bone surface	25.093	25.600	1.6041	21.3	28.5	26.600
Skin	6.497	6.450	0.5939	5.4	8.1	6.900
Upp. large int	0.000	0.000	0.0000	0.0	0.0	0.000
Thymus	0.580	0.600	0.2469	0.2	1.4	0.700
Oral mucosa	74.933	78.250	8.1290	47.9	86.4	80.525
Lymph	3.177	3.150	.5823	2.2	4.7	3.400
Eye lens	82.763	82.850	0.6128	81.5	83.7	83.250

Table (4.19) showed the organ dose estimated from The CT scanner Toshiba model Acquilion (16-slice) by CT Expo 2.5 software during this study:

	Mean	**Median**	**STD**	**Min**	**Max**	**Quartile**
Brain	42.467	42.900	0.8944	40.7	43.8	43.100
Salivary gland	43.330	50.100	12.1197	19.8	56.7	50.400
Thyroid	10.563	8.100	11.1293	3.2	58.3	13.200
Esophagus	0.378	0.400	0.2636	0.1	1.5	0.400
Lungs	0.281	0.300	0.2076	0.1	1.2	0.300
Bone marrow	6.270	6.400	.4471	5.6	7.6	6.400
Bone surface	15.881	16.400	1.4052	13.7	19.4	16.500
Skin	4.081	4.100	0.6196	3.4	6.4	4.400
Upp. large int	0.000	0.000	0.0000	0.0	0.0	0.000
Thymus	378	0.400	.2636	0.1	1.5	0.400
Oral mucosa	43.330	50.100	12.1197	19.8	59.7	50.400
Lymph	1.919	1.900	0.5671	1.2	3.8	2.200
Eye lens	53.222	53.300	0.4003	52.4	54.0	53.500

CHAPTER FIVE

DISCUSSION, CONCLUSION AND RECOMMENDATIONS

Chapter five

Discussion, Conclusion and Recommendations

5.1. Discussion:

In this study doses were expressed in terms of CTDIvol, DLP, and ED. This provide an indication of the average absorbed dose in the scanned region (CTDIvol), the integrated absorbed dose along a line parallel to the axis of rotation for the complete CT examination (DLP), and comparing the effective dose between tow CT scanner Toshiba machine, below we will discussion of the result in detail.

Table **(**4.1) and (4.5) from result represented the estimation of (mean, median, STD, min, max and 3 Quartile) and CTDI, DLP, E, PITCH calculated by software CT expo 2.5, were used data collection from CT scanner Toshiba ecquilion 64 slice both hospital (A) and (B) are used same protocol and show the both hospital have the same CTDI (79.2 mSv) and the same max DLP (1777.5 mSv/cm) and difference min DLP (1302.3 mSv/cm) and (1381.5 mSv/cm) for A and B hospital respectively, but the effective dose were difference between A and B hospital (3.2 to 8.0) mSv and (3.7 to 6.7) mSv respectively, although the max DLP for both hospital are the same but the max E are difference between A and B hospital because one DLP for male and other for female.

Table (4.9) and (4.13) from result represented the estimation of (mean, median, STD, min, max and 3 Quartile) and CTDI, DLP, E, PITCH calculated by software CT expo 2.5, were used data collection from CT scanner Toshiba ecquilion 16 slice both hospital (C) and (D) are used difference protocol and show the CTDI (50.9) mSv and (60.1) mSv and DLP (781.9 to 1240.2) mSv/cm and (1026.6 to 1209.9)

mSv/cm and E (1.9 to 5.9) mSv and (2.5 to 4.0) mSv for hospital (C) and (D) respectively , were the effective dose for hospital (C) are higher than hospital D although the hospital C use the lower CTDI than hospital D but the hospital D has higher DLP than hospital C, this difference refer to the area was irradiated.

For all hospital A, B, C and D in this study the effective dose for male are the lower than female although of constant parameter such as CTDI, DLP and this fact are presented in table (4.4), (4.8) for Toshiba 64 slice, were the effective dose for male she was 3.2 to 6.7 mSv and female 4.0 to 8.0 mSv, and table (4.12), (4.16) for Toshiba 16 slice the effective dose for male she was 2.0 to 3.7 mSv and female 1.9 to 5.9 mSv. This difference of effective dose for male and female refer to differ in composition of the tissue and weight.

Fieger (4.1) from results show the compare of effective dose between the four centers, were 4.6, 4.6, 2.8, and 3.3 mSv for centers A, B, C and D respectively, and show the mean effective dose in this study and were 3.8 mSv.

In general, the CTDI and DLP and E are the higher in Toshiba 64 slice than Toshiba 16 slice, this difference refers to increase in MAS for Toshiba 64.

In the table (4.17) were compering the mean of $CTDI_{vol,}$ DLP, and E, with Tanzania, Taiwan, United Kingdom and European Commission reference, was mean of CTDIvol, DLP, and E, was higher than Tanzania, Taiwan, United Kingdom and European Commission reference, and were compare the mean of effective dose in this study with local study in 2012 and were higher than them.

Table (4.18) & (4.19) from results show the organ doses for CT Toshiba 64 slice & 16 slice, some of this doses: Eye lens (82.8 ± 0.6) and (53.2 ± 0.4) mSv, salivary gland (74.9 ± 8.1) and (43.3 ± 12.1) mSv, brain (65 ± 1.6) and (42.5 ± 0.9) mSv, bone surface (25.1 ± 1.6) and (15.9 ± 1.4) mSv, thyroid (17.4 ± 14.4) and (10.6 ± 11.1) mSv, bone marrow (9.8 ± 0.5) and (6.3 ± 0.4) mSv respectively.

This result represents the organ dose in CT Toshiba 64 slice higher than CT Toshiba 16 slice, this difference refer to difference protocol are used.

5.2. Conclusion:

The aims of this study are determine the magnitude of radiation doses received by selected radiosensitive organ of the patients undergoing brain CT examination by two different CTMD, CT Toshiba 64 slice and CT Toshiba 16 slice and compare them. It was the organs doses in this study in CT Toshiba 64 slice are higher than organs doses in CT Toshiba 16 slice. It was the mean of effective dose to patients undergoing CT brain examination by CT Toshiba 64 slice are higher than mean of effective dose to patients undergoing CT brain examination by CT Toshiba 16 slice.

The effective dose in this study was compared them with different reported values from the Tanzania, Taiwan, United Kingdom, and EC reference and it was the highest effective dose. This difference in effective and organ doses refer to the difference in protocols.

5.3. Recommendations:

- Must using automatic mAs to achieve the optimization.
- Must reducing the scan range of the head so as to avoid the eye lens from exposure and thus reducing effective dose.
- recommend the results of this study are taken into consideration to increase interest in future study to confirm the differentiation between CTMD 64 slice and CTMD 16 slice in brain examination to achieve the lowest possible dose diagnosis.
- Must protect the eye from the radiation beam by the tilting the gantry to reduce eye lens dose.
- Optimization of protection should be conducted to the radiological departments by establishing standard protocol in the Sudan and commitment to quality control program.

References

ALI, M. 2005. Trends in CT abdominal doses in Malaysian practices.

ALLISY-ROBERTS, P. & WILLIAMS, J. R. 2007. *Farr's physics for medical imaging*, Elsevier Health Sciences.

ASSOCIATION, O. H. 2006. Computed tomography radiation safety issues in Ontario.

BASSIM, M. K., EBERT, C. S., SIT, R. C. & SENIOR, B. A. 2005. Radiation dose to the eyes and parotids during CT of the sinuses. *Otolaryngology-Head and Neck Surgery,* 133**,** 531-533.

BUSHBERG, J., SEIBERT, J., LEIDHOLDT JR, E. & BOONE, J. 2003. The essential physics of medical imaging. 2002. *Eur J Nucl Med Mol Imaging,* 30**,** 1713.

DANCE, D., CHRISTOFIDES, S., MAIDMENT, A., MCLEAN, I. & NG, K. 2014. Diagnostic radiology physics: A handbook for teachers and students. Endorsed by: American Association of Physicists in Medicine, Asia-Oceania Federation of Organizations for Medical Physics, European Federation of Organisations for Medical Physics.

HASSAN, O. A. M. 2012. *Estimation of Patient's Effective Dose during Routine Computed Tomography Examinations.* sudan university of science and technology.

JIBIRI, N. & ADEWALE, A. 2014. Estimation of radiation dose to the lens of eyes of patients undergoing cranial computed tomography in a teaching Hospital in Osun state, Nigeria. *International Journal of Radiation Research,* 12**,** 53.

KAINZ, K. 2006. Radiation oncology physics: a handbook for teachers and students. *Medical Physics,* 33**,** 1920-1920.

L.REDDINGER, W. 1997. CT Instrumentation and Physics.

MCCOLLOUGH, C., CODY, D., EDYVEAN, S., GEISE, R., GOULD, B., KEAT, N., HUDA, W., JUDY, P., KALENDER, W. & MCNITT-GRAY, M. 2008a. The measurement, reporting, and management of radiation dose in CT. *Report of AAPM Task Group,* 23**,** 1-28.

MCCOLLOUGH, C., CODY, D., EDYVEAN, S. & MEDICINE, A. A. O. P. I. 2008b. The measurement, reporting, and management of radiation dose in CT: report of AAPM task group 23 of the Diagnostic Imaging Council CT Committee. 2008. No. 96. *American Association of Physicists in Medicine (AAPM),* 96.

NGAILE, J. E. & MSAKI, P. K. 2006. Estimation of patient organ doses from CT examinations in Tanzania. *Journal of applied clinical medical physics,* 7**,** 80-94.

NIKUPAAVO, U., KAASALAINEN, T., REIJONEN, V., AHONEN, S.-M. & KORTESNIEMI, M. 2015. Lens dose in routine head CT: comparison of different optimization methods with anthropomorphic phantoms. *American Journal of Roentgenology,* 204**,** 117-123.

OSMAN, N. M. 2016. *Assessment of Radiation Dose for Patients Undergoing Brain and Abdomen Computed Tomography.* Sudan University of Science and Technology.

PODGORSAK, E. B. 2005. Radiation oncology physics. *Vienna: International Atomic Energy Agency***,** 123-271.

PRINS, R. D., THORNTON, R. H., SCHMIDTLEIN, C. R., QUINN, B., CHING, H. & DAUER, L. T. 2011. Estimating radiation effective doses from whole body computed tomography scans based on US soldier patient height and weight. *BMC medical imaging,* 11**,** 20.

PROTECTION, R. 2007. ICRP publication 103. *Ann ICRP,* 37**,** 2.

REHANI, M., CIRAJ-BJELAC, O., VAÑÓ, E., MILLER, D., WALSH, S., GIORDANO, B. & PERSLIDEN, J. 2010. Radiological protection in fluoroscopically guided procedures performed outside the imaging department. *Annals of the ICRP,* 40**,** 1-102.

SADRI, L., KHOSRAVI, H. & SETAYESHI, S. 2013. Assessment and evaluation of patient doses in adult common CT examinations towards establishing national diagnostic reference levels. *Int. J. Radiat. Res,* 11**,** 245-252.

SUZUKI, S., FURUI, S., ISHITAKE, T., ABE, T., MACHIDA, H., TAKEI, R., IBUKURO, K., WATANABE, A., KIDOUCHI, T. & NAKANO, Y. 2010. Lens exposure during brain scans using multidetector row CT scanners: methods for estimation of lens dose. *American Journal of Neuroradiology,* 31**,** 822-826.

TAN, J., TAN, K.-L., LEE, J., WAN, C.-M., LEONG, J.-L. & CHAN, L.-L. 2009. Comparison of eye lens dose on neuroimaging protocols between 16-and 64-section multidetector CT: achieving the lowest possible dose. *American Journal of Neuroradiology,* 30**,** 373-377.

VALENTIN, J. 2007. *The 2007 recommendations of the international commission on radiological protection*, Elsevier Oxford.

5.4 Appendix

Patient info.			Scan parameters											Console displayed dose	
NO	Sex M/F	Age	kV	(mA)	mAs	Slice thickness (mm)	pitch	Speed	Total scan time (s)	Number of slice	Table movement		Scan length (cm)	CTDIvol	DLP
											Start	End			
1															
2															
3															
4															
5															
6															
7															
8															
9															
10															
11															
12															
13															
14															